Synthesis of starburst hexa(oligoanilinated) C_{60} using hexanitro[60]fullerene as a precursor

Vijayaraj Anantharaj, Lee Y. Wang, Taizoon Canteenwala and Long Y. Chiang *

Center for Condensed Matter Sciences, National Taiwan University, Taipei 107, Taiwan

Received (in Cambridge, UK) 5th July 1999, Accepted 8th September 1999

Efficient syntheses of starburst hexaanilino, hexa(dianilino), hexa(tetraanilino), and hexa(hexadecaanilino)-[60]fullerenes (HHDAF) were demonstrated using hexanitro[60]fullerene (HNF) as a reactive precursor molecule. The tertiary nitro groups of HNF were found to act as excellent leaving groups for replacement by a nucleophilic substituent. Utilizing this reactivity with electron-donor nucleophiles, a synthetic approach was developed for the production of oligoanilinated fullerenes as intramolecular donor–acceptor A–$(D)_6$ starburst macromolecules with a well-defined arm number and chain length. The reactivity of HNF with oligomeric anilines increases with increasing number of repeating aniline units. Only an equal molar quantity of tetraaniline and hexadecaaniline was necessary for a complete reaction with HNF under mild conditions. The quantitative measurement of the material's proton counts over the ^{1}H NMR spectrum was utilized for determining the number of addends per C_{60} in the composition of oligoanilinated fullerenes. As a result, the NMR data fits well with the structure of tetraanilinated and hexadecaanilinated fullerenes, containing 6 tetraanilino and hexadecaanilino arms per C_{60}, respectively. This composition of HHDAF was also supported by the DCI$^-$-MS spectroscopic data showing an approximate correlation of the total relative peak intensities of fragmented oligoanilino mass ion groups. The optical properties of hexa(hexadecaanilino)[60]fullerenes revealed a close similarity with that of high molecular weight polyanilines.

Fullerene-derived polymers have great potential in the applications of biological[1] and material science, including their use in electroluminescent cells,[2] as polymer grid triodes,[3] photolithography medium,[4] optical limiting solids,[5] and photoinduced conductive materials.[6,7] A synthesis of C_{60}-containing star-shaped polymers has been demonstrated by the treatment of C_{60} with living polystyrene (PS^-)[8] or butyl-terminated polyacrylonitrile[9] (PAN) carbanions giving products of $C_{60}(PS)_x$ or polyacrylonitrilated C_{60}, respectively, with multiple polymer arms on each fullerene cage. An interesting anionic approach, which allows perfect control of the number of polymer chains added onto each fullerene molecule, was demonstrated using reactive living polystyryl and polyisoprene carbanions to afford hexa-adducts of grafted chains per C_{60} resulting in products with a well-defined composition of grafted polystyryl arms.[10,11]

It is possible to synthesize dendritic,[12] end-capped,[13] and star-shaped macromolecules[14] derived from C_{60} containing 6 or more polymer arms. Evidently, hexaanionic hexa(polystyryl)-fullerenes were found to be reactive enough for initiating polymerization of styrene and methyl methacrylate monomers.[15] Nevertheless, only one additional polystyrene arm can be attached on hexa(polystyryl)fullerenes forming hepta(polystyryl)fullerenes. The use of a free-radical method for copolymerization of C_{60} with styrene or methyl methacrylate (MMA) monomers often leads to complex polymer product mixtures.[16,17] However, in one case of MMA polymerization, only one C_{60} unit was estimated in each high molecular weight PMMA polymer molecule, forming a star-like structure with an average branch number of five per C_{60} over the entire molecular weight distribution.[18] The other synthesis of star-shaped polymers involved a polycondensation reaction of polyhydroxylated C_{60} with isocyanated prepolymers giving hexa-armed macromolecules.[14,19,20]

Here we report the first example of facile synthetic methods for the preparation of fullerene-derived rigid-rod starburst macromolecules, such as hexa(oligoanilinated)C_{60}, containing a well-defined number of rigid-rod arms per C_{60} using hexanitro[60]fullerene as a precursor reagent. By chemically attaching multiple oligoanilines onto a C_{60} molecular core, the resulting starburst poly(oligoanilinated) fullerenes may exhibit efficient three-dimensional intermolecular electron transport or hopping behavior among doped oligoanilino arms. This molecular system also allows us to investigate the intramolecular electron-transfer properties between oligoanilino donors and the fullerenic acceptor in the photo-activated state. The electronic conductive star polymers comprising rigid arms of the repeating conjugated monomer unit as their fundamental structure, may differ greatly from the conventional polymer containing a linear backbone of the same monomer, such as aniline, pyrrole, thiophene, or phenylenevinylene, in molecular packing and film morphology.[21] In addition, the molecular weight multiplication of starburst polymers becomes significant as the number of arms increases and may also greatly improve the mechanical properties of the final products compared with those of the parent rigid-rod arms.

Results and discussion

High molecular weight polyaniline (PANI)[22,23] exhibits several intrinsic chromogenic structures upon the treatment of either chemical oxidation or reduction, producing various compositions including blue protonated pemigraniline, violet pemigraniline base, blue emeraldine base, green protonated emeraldine, and colorless leucoemeraldine. Among these different forms, the protonated emeraldine base is a conductive material. Accordingly, switching the optical absorption and conductivity of polyaniline, upon structural interchange between its benzenoid and quinonoid-forms along the polymer chain, can be achieved simply by the reversible electrochemical redox and chemical protonation–deprotonation treatments. It was proposed that the electronic properties of polyaniline could be simulated using oligoaniline models, such as octaaniline in an intermediate emeraldine base oxidation state of B_5Q_2 (B denotes a benzenoid group and Q denotes a quinonoid group

in the backbone of oligoaniline).[24,25] Many studies of oligoanilines were thus prompted aiming to qualitatively reproduce the electronic conductivity of PANI in its low molecular weight version of oligomers.[26] Generation of appreciable conductivity with oligoanilines becomes possible when a proper oxidation state is made and protonated using a Brønsted acid.[24–27] The use of oligoaniline donor (D) as the component of star arms in connection with the fullerenic acceptor (A) core should lead to the corresponding electro- and photo-active A–$(D)_n$ macromolecules, partly resembling the electronic characteristics of PANI.

Fullerene molecules are highly reactive towards a great number of chemical reagents under various conditions.[28] However, synthetic methods suitable for the preparation of rigid-rod bound star polymers of fullerenes remain rare. Recently, we reported the synthesis and characterization of hexanitro[60]-fullerene (**1**, HNF), $C_{60}(NO_2)_6$, containing a well-defined number of addends using the radical addition of nitrogen dioxide as a nitration method.[29] Reactivity of fullerenic nitro groups in the structure of **1** is high even with weak nucleophiles,[30] such as H_2O, in a neutral solution at elevated temperatures. As the nucleophilicity of reactant increases, faster reaction kinetics are expected. A large increase in reactivity of primary organo-amines towards the replacement of fullerenic nitro groups overcomes the rate-retarding effect induced by the increasing structural complexity of the reactant. This improved precursor approach allows the attachment of multiple oligoanilines onto a C_{60} cage in a moderate to fast rate. In contrast, synthesis of oligoanilinated fullerenes was difficult using a direct addition reaction of C_{60} with oligoanilines even though fullerenes were reported to be reactive with some simple amines.[31,32]

The reaction of C_{60} in either toluene or benzene with gaseous $^{\bullet}NO_2$ at ambient temperature for a period of 3–4 h gave orange–red products of polynitrofullerenes in a high yield of more than 90%. Detailed conditions for the generation of nitrogen dioxide were described previously,[29] except a different temperature (40 °C) was used for the improvement of the HPLC results. A large excess of nitrogen dioxide promotes the formation of mononitrated and dinitrated toluene byproducts, as white crystals, at the benzyl carbon position. The degree of nitration was found to follow a stepwise manner with addition of two nitro groups at each step. At a reaction period of 3.0 h at 40 °C, tetranitro[60]fullerene (TNF), $C_{60}(NO_2)_4$, was the major product and dinitro[60]fullerene (DNF) and hexanitro[60]-fullerene were the minor products. The chromatographic peak corresponding to DNF diminished over a nitration period of 5.0 h and was accompanied with an increase in a comparable yield of hexanitro[60]fullerene (39%) and tetranitro[60]fullerene (47%), as shown in the second and third peaks of Fig. 1a, respectively. Consecutive addition of nitro groups onto TNF was detectable within a reaction period of 16 h as HNF becoming a major product and showed nearly a single peak in its chromatographic profile (Figs. 1b and 1c) at the end of reaction. These results demonstrated the feasibility of a complete nitration of C_{60} by an overnight reaction.

Structurally, most fullerenic nitro functional groups of polynitrofullerenes can be located at a tertiary benzyl carbon adjacent to extended olefins.[33,34] This particular hyperconjugated structure makes nitro groups act as potent leaving groups. Nucleophilic replacement of these nitro leaving groups by multi-functional heteroatom-containing alkoxy, thiol, and amino analogous nucleophiles may represent a facile synthetic method for the preparation of new polyfunctionalized fullerene derivatives and polymers. However, higher nucleophilicity of the applied reagent than that of water is essential to overcome the frequently occurring partial hydrolysis of **1** during the reaction. Hydrolytic side-reactions became negligible when primary organoamine compounds were used as nucleophiles under anhydrous conditions. Thus, amphiphilic aniline and polar oligo-

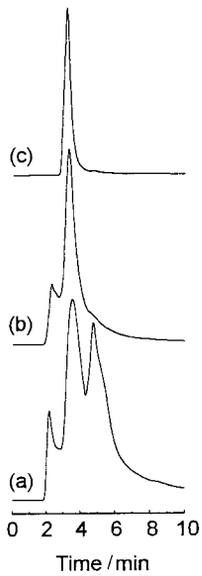

Fig. 1 HPLC profiles of the nitrated fullerene fractions synthesized by the reaction of C_{60} with $^{\bullet}NO_2$ at 40 °C for a reaction period of (a) 5.0 h, (b) 16 h, and (c) 16 h after purification by solvent washings, showing evolution of tetranitro[60]fullerene and hexanitro[60]fullerene fractions at a retention time of 4.77 and 3.53 min, respectively. The first fraction at a retention time of 2.17 min corresponds mainly to α-mononitrated and α,α′-dinitrated toluenes.

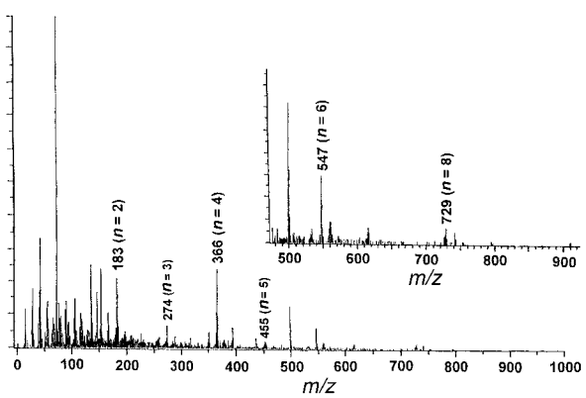

Fig. 2 Positive ion fast atom bombardment (FAB^+) mass spectrum (direct probe) of the neutralized tetraaniline product **6** synthesized from the oxidation of dianiline with ferric chloride, showing several consecutive fragmented mass groups corresponding to oligoaniline ions of $(aniline)_n^+$ with $n = 4$ (major), 6, and 8 (minor).

anilines readily attack **1** forming the corresponding starburst anilinated and oligoanilinated C_{60} molecules, respectively, without much complication by hydroxylated byproducts (Scheme 1). Complete substitution of all nitro groups in **1** by oligoanilines yielded the corresponding hexa(oligoanilino)[60]-fullerenes.

Oligoanilines were synthesized by the oxidative coupling reaction of anilines with an appropriate phenylamine or diamine.[26] In this study, the acid-doped tetraaniline was prepared by a reported method from *N*-(phenyl)phenylene-1,4-diamine (dianiline) using ferric chloride hexahydrate (1.0 equiv.) as an oxidant in aqueous HCl solution (0.1 M) at ambient temperature for 2.0 h, as shown in Scheme 1.[27] Positive ion fast atom bombardment (FAB^+) mass spectra (direct probe) of the neutralized products of tetraaniline, pre-treated by NH_4OH, showed several fragmented mass groups corresponding to oligoaniline ions of $C_6H_5NHC_6H_4NH^+$, $C_6H_5NH(C_6H_4NH)_3H^+$, $C_6H_5NH(C_6H_4NH)_5^+$, and $C_6H_5NH(C_6H_4NH)_7^+$ at *m/z* (relative intensity) 183 (21%), 366 (24%), 547 (6.0%), and 729 (1.3%), respectively, as depicted in Fig. 2. The data are indicative of the existence of an aniline hexamer and an octamer as minor products resulting from the oxidative

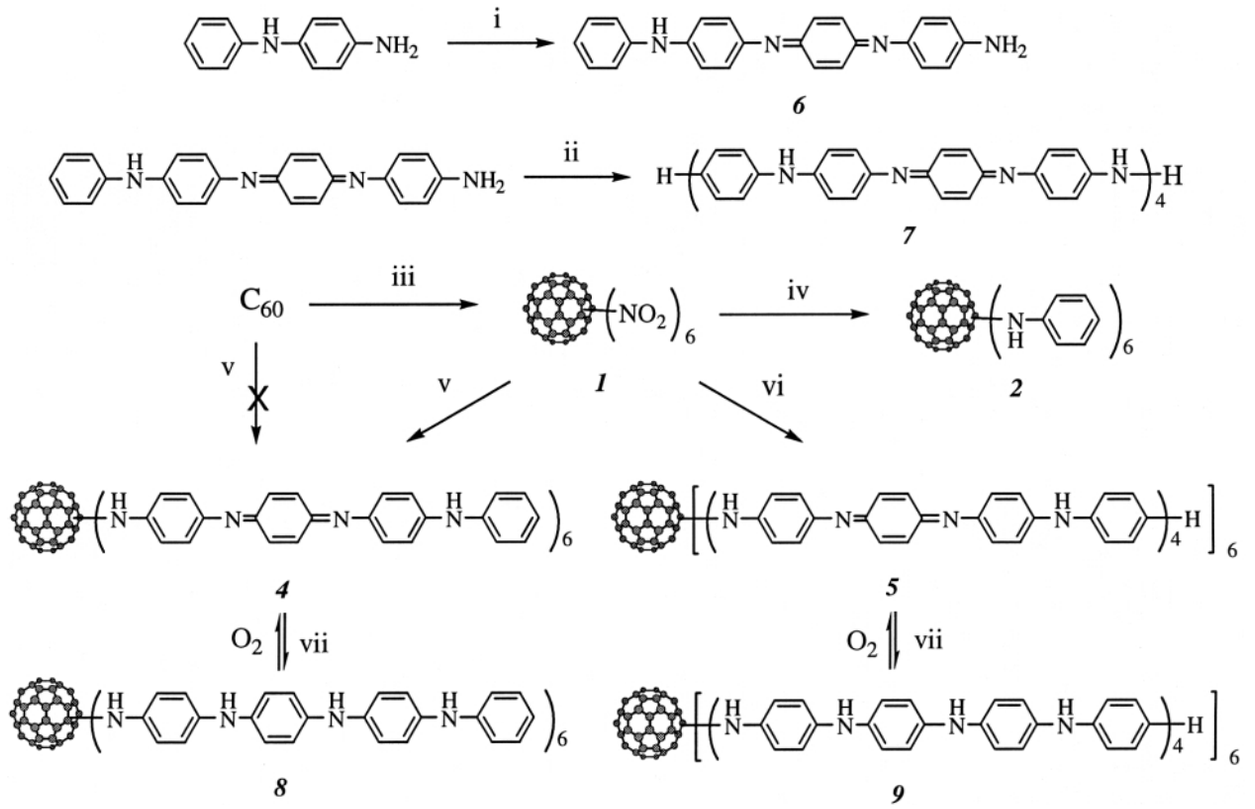

Scheme 1 *Reagents and conditions*: i, ferric chloride hexahydrate (1.0 equiv.), aq. HCl (0.1 M), r.t., 2.0 h, followed by NH_4OH; ii, $(NH_4)_2S_2O_8$ (1.5 equiv.), aq. HCl (0.1 M), r.t., 2.0 h, followed by NH_4OH; iii, gaseous $^{\bullet}NO_2$–N_2O_4 (from conc. HNO_3 and Cu powder), toluene, 60 °C, 5.0 h; iv, aniline (excess), Et_3N, THF, 50 °C, 6.0 h; v, tetraaniline (the emeraldine base form, excess), Et_3N, THF, 50 °C, 6.0 h; vi, hexadecaaniline (the emeraldine base form, excess), Et_3N, THF, 50 °C, 24 h; vii, NH_2NH_2, EtOH, DMF.

coupling reaction of the aniline dimer with ferric chloride, in addition to the major product of aniline tetramer. After further separation of the neutralized products on the thin layer chromatographic plates (TLC, SiO_2), tetraaniline **6** in its emeraldine oxidation state was isolated at $R_f = 0.5$ using EtOAc–hexane (1 : 1) or $R_f = 0.7$ using THF–$CHCl_3$ (1 : 1) as eluent.

The acid-doped hexadecaaniline was prepared by the reaction of tetraaniline in its leucoemeraldine oxidation state with $(NH_4)_2S_2O_8$ (1.5 equiv.) in aqueous HCl solution (0.1 M) at ambient temperature for 2.0 h.[27] Tetraaniline leucoemeraldine was made by the reduction of tetraaniline emeraldine with hydrazine (NH_2NH_2). After neutralization with NH_4OH and chromatographic isolation of the products on TLC (SiO_2), hexadecaaniline **7** was obtained at $R_f = 0.6$–0.75 using THF–$CHCl_3$ (1 : 1) as eluent. The negative ion desorption chemical ionization mass spectrum of **7** displayed a series of ion fragmentation groups with the mass of the highest ion peak in the group at *m*/*z* 366 ($n = 4$), 457 ($n = 5$), 548 ($n = 6$), 639 ($n = 7$), 730 ($n = 8$), 821 ($n = 9$), 911 ($n = 10$), 1002 ($n = 11$), 1092 ($n = 12$), 1183 ($n = 13$), 1274 ($n = 14$), and 1454 ($n = 16$), corresponding to $(aniline)_n$ ions.[35] The ions with a mass lower than that of aniline decamer correspond well with the molecular weight of the corresponding oligoaniline in the leucoemeraldine state. A slight increase of 1–2 quinonoid aniline units (Q, $=C_6H_4=$) per oligoaniline chain was detected in the higher mass ions. Preservation of the quinonoid aniline structure during fragmentation became more obvious in the matrix-assisted laser desorption ionization (MALDI) mass spectrum of **7**. It showed a similar series of ion fragmentation groups in the higher mass region than *m*/*z* 700 with the mass of the highest ion peak in each fragmented group at *m*/*z* 726 $[H(C_6H_4NH)_8H - 4H]$, 816 $[H(C_6H_4NH)_9H - 5H]$, 907 $[H(C_6H_4NH)_{10}H - 5H]$, 998 $[H(C_6H_4NH)_{11}H - 5H]$, 1087 $[H(C_6H_4NH)_{12}H - 7H]$, 1179 $[H(C_6H_4NH)_{13}H - 6H]$, 1269 $[H(C_6H_4NH)_{14}H - 7H]$, 1359 $[H(C_6H_4NH)_{15}H - 8H]$, 1450 $[H(C_6H_4NH)_{16}H - 8H]$, 1540 $[H(C_6H_4NH)_{17}H - 9H]$, and 1630 $[H(C_6H_4NH)_{18}H - 10H]$.[35] A progressive increase in the number of the quinonoid aniline units per chain of oligoaniline was detected as its molecular weight increases and the mass of the highest ion peak in the group shifts away from the mass of its leucoemeraldine analogue. Accordingly, the mass of octaaniline, dodecaaniline, and hexadecaaniline ions showed a 4, 6–7, and 8 mass unit, respectively, lower than the molecular weight of the corresponding oligoaniline leucoemeraldine. The difference in mass can be correlated well with a total of 2, 3, and 4 quinonoid aniline units, on average, in octaaniline, dodecaaniline, and hexadecaaniline ions as B_5Q_2, B_8Q_3, and $B_{11}Q_4$ (B denotes a benzenoid group, $–C_6H_4–$, in the backbone of the oligoaniline), respectively. This MALDI-MS data provided evidence for the existence of hexadecaaniline emeraldine **7**, as the average structure shown in Scheme 1, in a higher probability than other oxidation states of the compound. It also indicated several mass groups with a relatively low peak intensity and with a higher mass up to $(aniline)_{20}$ as conceivable minor products.

Unlike other aliphatic nitro compounds, the fullerenic carbon–nitro bonding is rather weak and vulnerable to nucleophilic replacement and rearrangement in solution at ambient temperature. Its stability increases sharply in the solid state at 0 °C. This type of nitro group can be replaced over an extended period of time by water molecules forming partially hydroxylated nitrofullerene derivatives.[30] Upon treatment of $C_{60}(NO_2)_6$ in THF with an excess of freshly distilled aniline in the presence of triethylamine at 50 °C for 6.0 h under N_2, hexaanilino[60]-fullerene (HAF, **2**) was obtained as a major product (brown solids) in 94% yield. Separation of the compound **2** from the reaction medium was achieved by precipitation and repeated washings with hexane and was accompanied with removal of unreacted aniline, Et_3N, and other byproducts. Further purification of **2** was performed on thin-layer chromatographic plates (TLC, SiO_2) at $R_f = 0.76$ using a mixture of THF–$CHCl_3$ (1 : 1) as eluent.

Similar reaction conditions were applied for the synthesis of hexa(dianilino)[60]fullerenes (HDAF, **3**) using *N*-(phenyl)-phenylene-1,4-diamine as a nucleophilic reagent in the reaction with $C_{60}(NO_2)_6$ to afford desirable products in 76% yield after chromatographic purification on TLC. Compound **3** is highly soluble in DMF. In the case of aniline tetramer and hexadecamer, their nucleophilic substitution reactions with $C_{60}(NO_2)_6$ were found to be much more efficient than the corresponding reaction with aniline and dianiline. Only one equivalent quantity of tetraaniline or hexadecaaniline per nitro group of HNF was necessary to achieve completion of the reaction in the presence of triethylamine in THF at 50 °C for 6 h or longer. In this reaction, a co-solvent of *N*-methylpyrrolidinone (NMP) was used for enhancing the solubility of hexadecaaniline in THF prior to the reaction with **1**. Utilization of the co-solvent was also advantageous for preventing precipitation of the partially hexadecaanilinated fullerene intermediates during the reaction. A longer reaction period of 24 h was applied for the reaction with **7** than that for tetraaniline (6.0 h). At the end of the reaction, NMP was removed easily from the products upon the addition of water and this also caused precipitation of hexadecaanilinated fullerenes from the medium. The solid products were subsequently washed with either ether or acetonitrile for removal of the remaining unreacted tetraaniline or hexadecaaniline, respectively. Hexa(tetraanilino)[60]-fullerene (HTAF, **4**) and hexa(hexadecaanilino)[60]fullerene (HHDAF, **5**) were obtained as dark blue to violet solids in 72 and 94% yield, respectively. A large difference in solubility between **4** and **6** as well as **5** and **7** in THF allowed further removal of the starting monomers from the solid products.

Appreciable solubility of **5** in NMP and a mixture of NMP–THF made its chromatographic purification possible on TLC [SiO_2, $R_f = 0.7$ for **6** and $R_f = 0.1$ for **4** and **5** using THF–$CHCl_3$ (1 : 1) as eluent or $R_f = 0.9$ for **7** and $R_f = 0.2$ for **5** using THF–$CHCl_3$ (3 : 1) as eluent]. All products of **2**, **3**, **4**, and **5** displayed a sharp single chromatographic peak in their HPLC profile using a reverse-phase MCH-5 column and acetonitrile as eluent, as shown in Fig. 3. A relatively high purity in terms of the composition of these starburst molecules was confirmed. The retention times of **4** (3.9 min) and **5** (4.0 min) were found to be lower in value than those of **2** (4.5 min) and **3** (4.45 min), indicating a slightly higher polarity for **4** and **5**. Furthermore, a limited solubility of HHDAF in acetonitrile resulted in a high baseline fluctuation of the HPLC profile (Fig. 3d).

Multiple additions of aniline units on each C_{60} molecule were evident as the negative ion desorption chemical ionization mass spectrum (DCI$^-$-MS, direct probe) of **2** gave a clear spectrum profile showing a series of ion fragmentation groups. Each group consists of several ion peaks with the mass of the peak in the highest intensity in the group at *m*/*z* 813 ($n = 1$), 904 ($n = 2$), 995 ($n = 3$), 1086 ($n = 4$), and 1177 ($n = 5$), as shown in Fig. 4. The mass group containing the molecular ion of **2** at *m*/*z* 1272 ($n = 6$) falls within the baseline noise. A progressive increase of nearly constant 91 mass units from the parent C_{60} ion peak at *m*/*z* 721 was observed. These ion fragmentations gain a deprotonated aniline (C_6H_5N) functional group with respect to the preceding ion fragment and agree well with the mass of $C_{60}(NC_6H_5)_n^-$ that can be correlated to the polyanilino[60]fullerene ions consistent with the composition of **2**.

In the case of HHDAF, rapid cleavage of all fullerene–hexadecaaniline bonds attached on a C_{60} cage was observed under mass spectroscopic conditions. Consequently, the negative ion DCI mass spectrum of **5** (Fig. 5) exhibited a strong peak at *m*/*z* 721 corresponding to the mass of the C_{60} ion fragment and a series of ion fragmentations at *m*/*z* (with the relative percentage group intensity indicated) 548 ($n = 6$, 18.5%), 637 ($n = 7$, 22.3), 728 ($n = 8$, 30.4), 820 ($n = 9$, 54.7), 912 ($n = 10$, 71.6), 1003 ($n = 11$, 80.5), 1093 ($n = 12$, 67.6), 1185 ($n = 13$, 80.8), 1276 ($n = 14$, 29.9), 1367 ($n = 15$, 16.6), and 1459 ($n = 16$, 12.5). These ion fragments correspond well to a consecutive

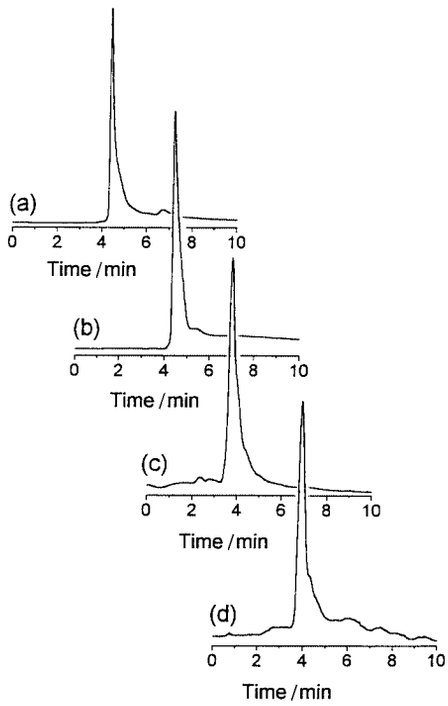

Fig. 3 HPLC chromatographic profile of (a) hexaanilino[60]fullerene **2**, (b) hexa(dianilino)[60]fullerene **3**, (c) hexa(tetraanilino)[60]fullerene **4**, and (d) hexa(hexadecaanilino)[60]fullerene **5**, showing a narrow distribution of products. The measurements were carried out using a reverse-phase MCH-5 column with acetonitrile as eluent and a flow rate of 0.6 ml min^{-1}.

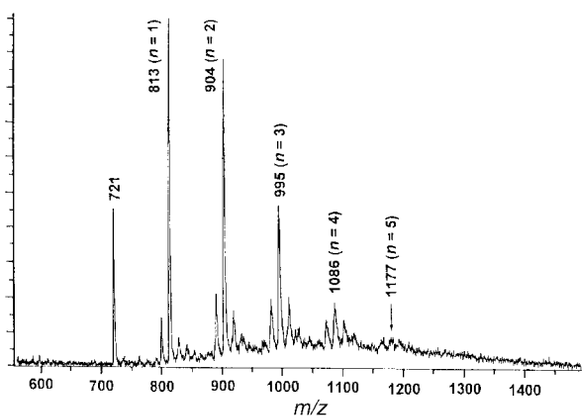

Fig. 4 Negative ion desorption chemical ionization (DCI$^-$) mass spectrum of hexaanilino[60]fullerene **2** showing a consecutive fragmentation of $C_{60}(aniline)_n$ ions.

fragmentation of hexadecaaniline ions, $H(C_6H_4NH)_n^-$, from $n = 16$ to 6. The spectrum also showed the other series of ion fragmentations at *m*/*z* (with the relative percentage group intensity indicated) 561 ($n = 6$, 28.5%), 653 ($n = 7$, 38.2), 744 ($n = 8$, 47.5), 835 ($n = 9$, 71.5), 927 ($n = 10$, 100), 1018 ($n = 11$, 70.6), 1110 ($n = 12$, 43.8), 1200 ($n = 13$, 26.5), 1292 ($n = 14$, 20.6), 1383 ($n = 15$, 14.1), and 1475 ($n = 16$, 10.9), corresponding to consecutive fragmentation of $HN(C_6H_4NH)_nH^-$ ions from $n = 16$ to 6. The total relative peak intensity of the first and second series of ion fragmentations was found to be 485.5% and 472.2%, respectively. Each starburst macromolecule **5** consists of one C_{60} cage and 6 hexadecaanilino arms. The value of each total intensity of the ion mass series is 5.6–5.7-fold higher than that of the C_{60} ion peak (85.1%). The nearly equal total relative intensity of $H(C_6H_4NH)_n^-$ and $HN(C_6H_4NH)_nH^-$ ions also implied a 50% cleavage of the aniline–phenyl bond at the end group of the chain during the DCI-MS measurements. Fragmentation of each hexadecaanilino arm should produce

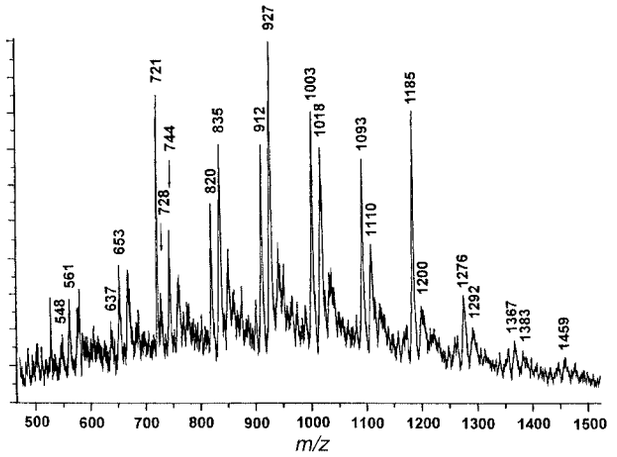

Fig. 5 Negative ion desorption chemical ionization (DCI^-) mass spectrum of hexa(hexadecaanilino)[60]fullerene **5**, showing a mass ion of the C_{60} fragment at *m/z* 721 and a consecutive fragmentation of hexadecaaniline ions, $H(C_6H_4NH)_n^-$, and $HN(C_6H_4NH)_nH^-$, from n = 16 to 6.

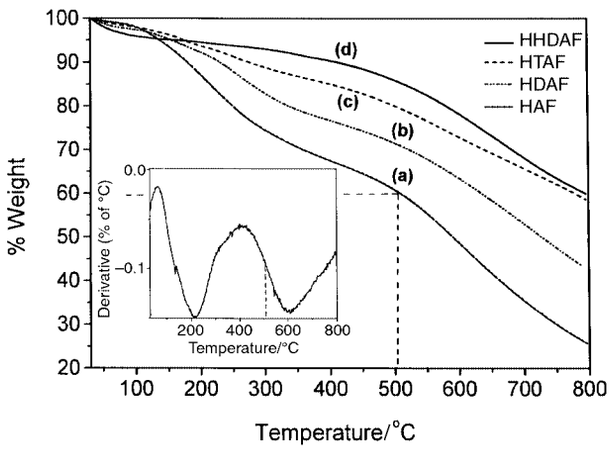

Fig. 6 Thermogravimetric profiles of (a) hexaanilino[60]fullerene (**2**, HAF), (b) hexa(dianilino)[60]fullerene (**3**, HDAF), (c) hexa(tetraanilino)[60]fullerene (**4**, HTAF), and (d) hexa(hexadecaanilino)[60]fullerene (**5**, HHDAF) under N_2. The insert shows the derivative peak of the percentage weight loss profile (a). The heating rate was 5 °C min^{-1} for HAF and 10 °C min^{-1} for HDAF, HTAF, and HHDAF.

two smaller mass ions in a similar intensity and *vice versa* for the recombination of ion masses. Therefore, when all smaller peaks are also counted, the sum of all relative group peak intensities in the two series of ion mass groups approximately support the composition of HHDAF.

The thermal stability of oligoanilinated fullerenes remains excellent at temperatures below 500 °C as the molecular weight of oligoaniline is increased to over 1400 Daltons. For a low molecular weight HAF compound, a sharp rate of weight loss was observed at temperatures above 150 °C, as shown in Fig. 6. The HAF profile was divided into three regions of thermal degradation each with a different rate of weight loss at temperatures of 150–300, 300–520, and 520–800 °C. Interestingly, at the turning-point temperature of 500 °C between the second and third regions, the total weight loss of **2** was estimated to be 40% which matches approximately the percentage weight ratio of 6 aniline moieties in **2** (43%), consistent with its composition. This temperature was measured at the half height of the derivative peak of the percentage weight loss profile, as shown in the insert of Fig. 6. High thermal stability of the fullerene cage coupled with simple aromatic aniline addends may allow HAF to release aniline moieties gradually upon heating before reaching a temperature range capable of producing a deflated carbon cage at 500–600 °C. However, possible formation of complex thermal intermediates at high temperatures cannot be ruled out.

As the number of repeating aniline units of each attached arm increases, the percentage weight loss of material at 500 °C decreases to 29, 21, and only 14% for HDAF, HTAF, and HHDAF, respectively. The TGA profile of HHDAF was associated with a slow weight loss rate of 0.025% per °C, substantially lower than that of **2** (0.1% per °C) at temperatures between 100 and 500 °C. Above 500 °C, the rate of weight loss increases for all samples. However, a retention of 58% by weight of material for both HHDAF and HTAF was possible at a temperature as high as 800 °C. At this thermal stage, formation of extended carbonaceous networks induced by the intermolecular coupling of fullerenic radicals is proposed. The observed high thermal stability in addition to solubility of HHDAF and HTAF may provide certain advantages in materials processing and applications over PANI.

The other prominent method for determining the number of addends per C_{60} molecule in the composition of fullerene derivatives is to make the quantitative measurement of the materials proton count *via* the proton integration over its ^1H NMR spectrum. The actual molarity of each type of proton in a compound can be correlated and estimated from the integration ratio of protons at a different chemical shift, using an internal standard reference in a known quantity (moles) for calibration. In this case, 1,4-diazabicyclo[2.2.2]octane (Dabco, 30–50 μmol) was applied as an internal reference in all NMR measurements. A sharp, singlet proton peak of Dabco at a chemical shift of δ 2.60 does not interfere with any of the oligoanilinic protons in the region of δ 4.0–8.0. A reasonable accuracy in determining the number of each type of proton per molecule was demonstrated using a pre-calculated amount (moles) of dianiline *vs.* Dabco in a model test.

The emeraldine base tetraaniline **6** exists in three resonance forms which differ from each other only in the location of the quinonoid (Q) unit. In the structure of each tautomer, three types of carbon protons, namely, end-group phenyl protons H_a and H_b, phenyl protons H_c *ortho* to the amino group, and quinonoid protons H_d, were categorized. Multiple proton peaks of H_b, H_c, and H_d with a doublet coupling splitting and a slight shift of the peak position from each other are possible due to the unsymmetrical nature of these protons. However, the overall relative proton ratio between each proton category of H_a/H_b, H_c, and H_d was estimated by integration over their characteristic range of chemical shifts at δ 6.45–6.68, 6.74–7.04, and 7.08–7.26, respectively, as shown in Figs. 7a and 7b. These three plausible isomeric structures of emeraldine base (EB) tetraaniline are depicted as $\mathbf{6}_a$, $\mathbf{6}_b$, and $\mathbf{6}_c$ with the quinonoid moiety being shifted by one aniline unit. Co-existence of three isomers was evident as revealed by the ^1H NMR spectrum of the product. The relative ratio between isomers changes upon prolonged storage. As shown in Fig. 7a, the initial product composition of **6** freshly isolated from the reaction consisted of an appreciable percentage (22% based on the proton integration ratio of the terminal N–H proton peaks) of $\mathbf{6}_c$. The compound $\mathbf{6}_c$ contains a quinonoid moiety as an end-group and exhibits the terminal quinonoid amino proton (H_{f3}) peak at the most

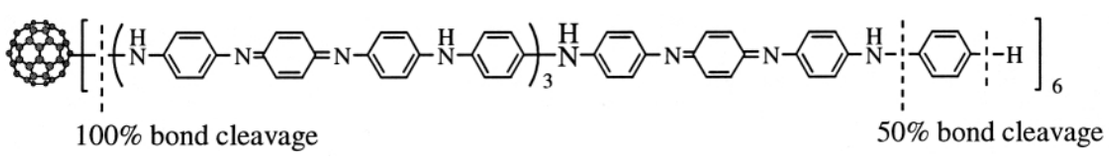

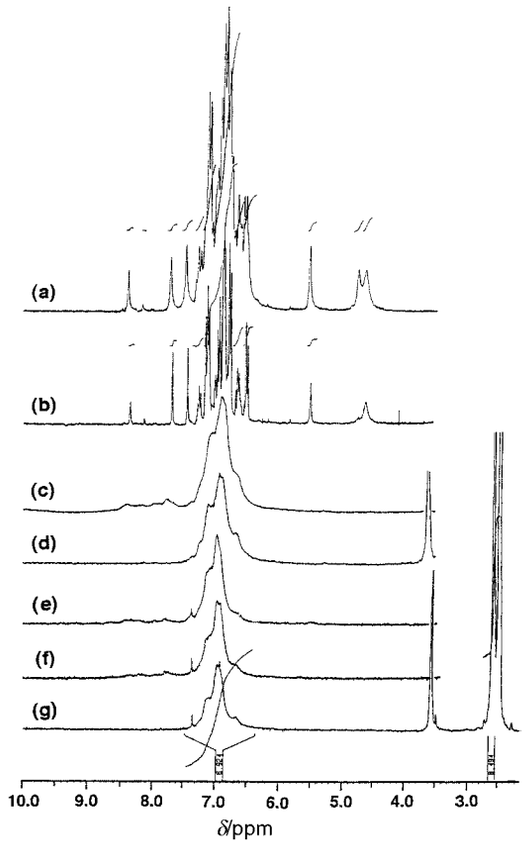

Fig. 7 ^{1}H NMR spectra (DMSO-d_6) of (a) tetraaniline **6** (purified on pyridine pre-treated TLC, SiO_2), (b) tetraaniline **6** after storage at 5 °C for two weeks, (c) hexa(tetraanilino)[60]fullerene **4**, (d) **4** treated with D_2O, (e) hexadecaaniline **7**, (f) hexa(hexadecaanilino)[60]fullerene **5**, and (g) **5** treated with D_2O. A proton peak at δ 2.60 of Dabco was used as an internal reference for the proton counting.

down-field chemical shift of δ 8.35. The relative intensity of this peak decreased significantly as the thermal equilibration between the isomers was allowed for a period of roughly a week at ambient temperature or two weeks at 5 °C. At the equilibrium state, the ^{1}H NMR spectrum (Fig. 7b) of EB tetraaniline displayed groups of sharp peaks that allowed a better evaluation of the isomer distribution. Attempted isolation of a single isomer of **6** on a thin layer chromatographic plate (TLC) was not successful. Reisomerization of a TLC-isolated isomer back to a mixture of $\mathbf{6}_{a-c}$ isomers with a ratio similar to the one shown at the equilibrium state was observed by ^{1}H NMR (in close resemblance to that of Fig. 7b).

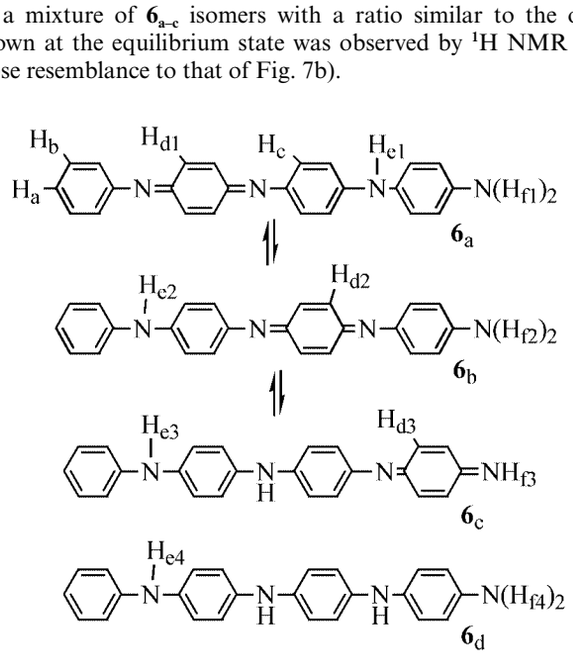

We assign the singlet peaks at δ 7.43 and 7.67 to the in-chain N–H_e amino protons of $\mathbf{6}_{a-c}$. The terminal benzenoid amino proton peaks of H_{f1} and H_{f2} were located at δ 4.62 and 5.49. Two groups of proton peaks (doublet-doublet) centered at δ 7.25 (H_{d3}) and 7.10 (H_{d1} and H_{d2}) correspond to the chemical shift of the end-group quinonoid C–H protons of $\mathbf{6}_c$ and the in-chain quinonoid C–H protons of $\mathbf{6}_a$ and $\mathbf{6}_b$, respectively. The relative peak intensities of these two groups of peaks indicated a percentage content of $\mathbf{6}_c$ as 13% of the total isomer composition of **6**.

To differentiate further the chemical shift of amino protons in $\mathbf{6}_a$ and $\mathbf{6}_b$, compound **6** was first chemically reduced by phenylhydrazine to $\mathbf{6}_d$, then re-oxidized by benzoquinone to **6** in an EB form. A sharp, singlet peak at δ 7.36 (H_{e4}) and a broad band centered at δ 4.6 (H_{f4}) were detected in the ^{1}H NMR spectrum of $\mathbf{6}_d$, corresponding to the chemical shift of the in-chain N–H and the end-group NH_2 protons, respectively. Re-oxidation of $\mathbf{6}_d$ caused suppression of the singlet H_{e4} peak that was accompanied with a new sharp singlet peak at δ 5.75. This new peak is assigned to the chemical shift of H_{f2} since the chemical shift of H_{f1} should more closely resemble that of H_{f4} in a reduced form. Based on these proton assignments, the integration ratio of two amino proton peaks at δ 4.62 and 5.49 in Fig. 7b may be correlated to the composition ratio of $\mathbf{6}_a$ and $\mathbf{6}_b$ as 61 and 26%, respectively, at the thermal equilibrium state.

The extension of aniline units going from aniline tetramer **6** to hexadecamer **7** (Fig. 7e) causes no obvious change of the characteristic chemical shift of each proton category H_a/H_b, H_c, and H_d, except all C–H and amino proton peaks are largely broadened. Evidently, the relative ratio of the end-group phenyl protons at δ 6.45 *vs.* the phenyl protons *ortho* to the amino group of **7** at δ 6.74–7.04 was found to be roughly 65% smaller than the corresponding ratio of **6**, consistent with the extended chain length of **7**. Conversely, the relative peak intensity of quinonoid protons of **7** at δ 7.08–7.26 remained nearly constant indicating a proportional increase of quinonoid moieties in the oligomer chain as the total number of aniline units increased. This also agrees well with the emeraldine structure of **7**. As multiple tetraaniline and hexadecaaniline arms were attached onto C_{60} forming the corresponding starburst macromolecules of **4** and **5**, respectively, a certain degree of proton peak broadening was observed, as shown in Figs. 7c and 7f. It was due partly to the increasingly complex environment surrounding each proton and the possibility of radical formation on the fullerene cage. Especially, even with a single residual radical on C_{60}, resulted from the plausible electron transfer from the donor arms to the acceptor core, the resolution of the NMR measurements can be disrupted greatly. Nevertheless, the relative proton peak intensity of each proton category H_a/H_b, H_c, and H_d remains accountable in the region of δ 6.0–7.5.

The relative proton integration count over a chemical shift range of δ 6.0–7.5 for all spectra of Fig. 7 was calibrated using an internal standard proton peak of Dabco at δ 2.60 as shown in Fig. 7g. Either the molecular weight or the total number of protons per molecule of substance can be calculated based on the formula in eqn. (1) where N_p, I_F, M_F, and m_F are the number

$$\frac{I_F M_F}{N_p m_F} = \frac{I_D M_D}{12\, m_D} \qquad (1)$$

of protons per molecule, proton integration, molecular weight, and the sample mass (mg), respectively, of the starburst fullerene compound applied. Whereas I_D, M_D, and m_D are the proton integration, molecular weight, and the sample mass (mg), respectively, of Dabco applied.

The structural inter-conversion between the benzenoid form and the quinonoid form of oligoanilino units upon exposure of **4** and **5** to redox conditions will not change the total number of aromatic C–H protons in the molecule. Therefore, regardless of the oxidation state of each oligoanilino arm, the sum of

Table 1 Estimation of the molecular weight of starburst fullerene compounds based on the proton integration ratio in the ^{1}H NMR spectra (DMSO-d_6) of Fig. 7, using Dabco as an internal standard for the determination of the proton count

Sample	Molecular formula[a]	Number of carbon protons per molecule (N_p)	Molecular wt. (theoretical)	Molecular wt. (observed, M_F, m.u.)
6	$(aniline)_4$	17	366 m.u.	363 (−0.8%)[b]
4	$C_{60}[(aniline)_4]_3$, $\mathbf{4}_3$	51	1815 m.u.	1455 (−19.8%)
4	$C_{60}[(aniline)_4]_4$, $\mathbf{4}_4$	68	2180 m.u.	1863 (−14.5%)
4	$C_{60}[(aniline)_4]_5$, $\mathbf{4}_5$	85	2545 m.u.	2329 (−8.5%)
4	$C_{60}[(aniline)_4]_6$, $\mathbf{4}_6$	102	2910 m.u.	2795 (−4.0%)
7	$(aniline)_{16}$	65	1458 m.u.	1489 (0.2%)
5	$C_{60}[(aniline)_{16}]_3$, $\mathbf{5}_3$	195	5091 m.u.	4703 (−7.6%)
5	$C_{60}[(aniline)_{16}]_4$, $\mathbf{5}_4$	260	6548 m.u.	6271 (−4.2%)
5	$C_{60}[(aniline)_{16}]_5$, $\mathbf{5}_5$	325	8005 m.u.	7838 (−2.1%)
5	$C_{60}[(aniline)_{16}]_6$, $\mathbf{5}_6$	390	9462 m.u.	9406 (−0.6%)

[a] An emeraldine base form of each oligoanilino arm was considered. [b] Percentage of deviation (observed molecular wt. − theoretical molecular wt.)/theoretical molecular wt., as an average of three samples.

integration over the chemical shift range covering all aromatic protons should allow one to estimate the total number of carbon protons per molecule. This can be correlated to the number of oligoanilino arms per starburst molecule. Consequently, with the known value of m_F, M_D and m_D and the measured value of I_F and I_D, the relationship between N_p and M_F can be determined and calculated *via* Equation (1). Assuming the number of oligoanilino arms of **4** and **5** is either **5** or **6** with a formula of $C_{60}[(aniline)_4]_5$ and $C_{60}[(aniline)_{16}]_5$ or $C_{60}[(aniline)_4]_6$ and $C_{60}[(aniline)_{16}]_6$, respectively, the calculated total number of carbon protons (N_p) per molecule and the theoretical molecular weight are summarized in Table 1. Based on the relative proton integration (I_D and I_F) obtained from all spectra in Fig. 7 and Equation (1), the observed molecular weight (M_F) was determined.

The accuracy in predicting the molecular weight of a macromolecule was evaluated with linear oligoanilines **6** and **7**. As shown in Table 1, the percentage deviation of the observed molecular weight from the theoretical one was found to be −0.8 and 0.2% for aniline tetramer and hexadecamer, respectively, within nearly the quantitative prediction of the molecular weight. In the case of a test sample of **4**, several experimental molecular weights M_F were estimated from Equation (1) using the same observed proton integration data and the number of carbon protons per molecule (N_p), based on the assumption of a series of plausible compositions of **4** as $C_{60}[(aniline)_4]_3$ ($\mathbf{4}_3$), $C_{60}[(aniline)_4]_4$ ($\mathbf{4}_4$), $C_{60}[(aniline)_4]_5$ ($\mathbf{4}_5$), or $C_{60}[(aniline)_4]_6$ ($\mathbf{4}_6$). To facilitate a clear counting of all carbon protons in **4** and **5**, the sample was treated with D_2O overnight to remove all the amino proton peaks, as shown in Figs. 7d and 7g. As a result, the percentage molecular weight deviation of the observed values from the theoretical values was found to increase (disregard the sign) systematically from −4.0, −8.5, −14.5 to −19.8% when the number of attached tetraanilino arms applied in the calculation of the theoretical molecular weight decreases from 6, 5, 4 to 3, respectively. Obviously, the NMR data in Fig. 7d fits well with the proton count of $\mathbf{4}_6$, containing 6 tetraanilino arms per C_{60}, with the lowest deviation. A similar practice was carried out on HHDAF samples. Based on the proton integration ratio between the sample **5** and Dabco obtained from the spectrum in Fig. 7g, the percentage of the molecular weight deviation increased (disregard the sign) from −0.6, −2.1, −4.2, to −7.6% of the theoretical value when the number of attached hexadecaanilino arms in **5** decreases from 6 for $C_{60}[(aniline)_{16}]_6$ ($\mathbf{5}_6$), 5 for $C_{60}[(aniline)_{16}]_5$ ($\mathbf{5}_5$), 4 for $C_{60}[(aniline)_{16}]_4$ ($\mathbf{5}_4$), to 3 for $C_{60}[(aniline)_{16}]_3$ ($\mathbf{5}_3$), respectively. Even though the absolute deviation becomes relatively smaller for the latter case, a systematic trend exists with the lowest deviation in favor of $\mathbf{5}_6$, containing 6 hexadecaanilino arms per C_{60}.

Infrared absorption of HTAF (Fig. 8b) and HHDAF (Fig. 8d) bore a close resemblance to that of the corresponding arms of **6** (Fig. 8a) and **7** (Fig. 8c) respectively. Clearly, IR absorption contributed from the fullerene moiety is not visible. The absorption of oligoanilino arms dominates the spectrum of HTAF and HHDAF. The UV–VIS spectrum (Fig. 9b) of **2** showed a band centered at 242 nm with a tail extending to roughly 500 nm, as a characteristic absorption of fullerene derivatives, and a broad shoulder band centered at 290 nm. The spectrum was compared with that of aniline, *N*-methylaniline, and hexa(*n*-butylamino)[60]fullerene, synthesized by the reaction of $C_{60}(NO_2)_6$ with *n*-butylamine. The two former compounds exhibit two bands centered at 250 and 292 nm for aniline (Fig. 9c) and at 248 and 299 nm for *N*-methylaniline (Fig. 9d) with no absorption at a wavelength longer than 330 nm. It indicates a change of the relative intensity of the second band at 299 nm to a lower wavelength when aniline is alkylated. This may also be the case for aniline moieties of **2**. Meanwhile, the band at 242 nm in the spectrum of **2** can be rationalized as the combined absorption of both the fullerene cage and anilino moieties, where the weak shoulder band at 290 nm in the same spectrum arises mainly from the absorption of anilino moieties. In principle, deduction of all UV absorptions of anilino

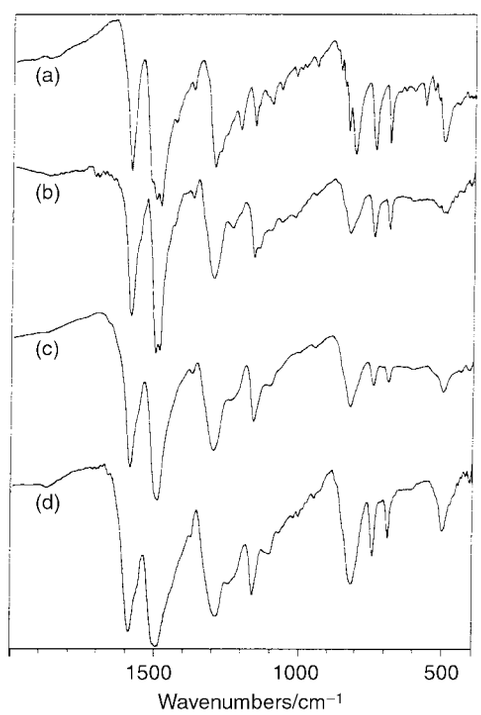

Fig. 8 Infrared spectra (KBr) of (a) tetraaniline **6**, (b) hexa(tetraanilino)[60]fullerene (HTAF), (c) hexadecaaniline **7**, and (d) hexa(hexadecaanilino)[60]fullerene (HHDAF).

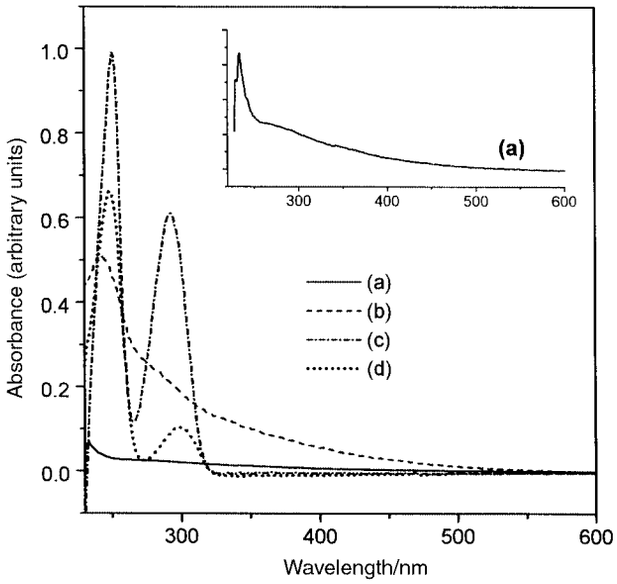

Fig. 9 UV–VIS spectra of (a) hexa(*n*-butylamino)[60]fullerene, (b) hexaanilino[60]fullerene **2**, (c) aniline, and (d) *N*-methylaniline in a concentration of 2.5×10^{-6} M in THF.

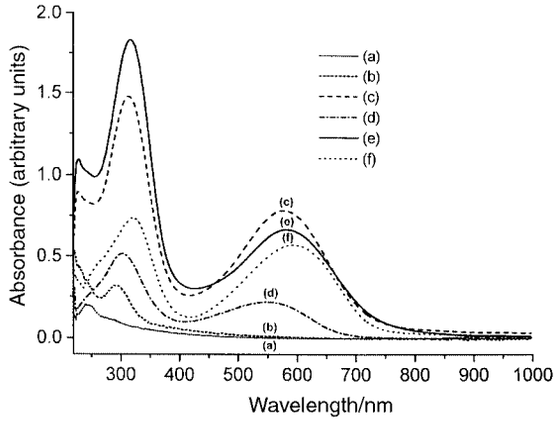

Fig. 10 UV–VIS spectra of (a) HAF **2**, (b) HDAF **3**, (c) hexadecaaniline **7**, (d) HTAF **4**, (e) HHDAF **5**, and (f) polyanilines (PANI) in a high molecular weight. The spectra of (a)–(e) were collected in a concentration of 2.5×10^{-6} M in THF.

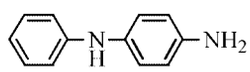

(the B-form of dianiline)

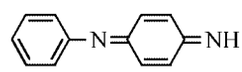

(the Q-form of dianiline)

moieties from the spectrum of **2** should lead to a remaining absorption profile of the fullerene moiety, resembling that of hexa(*n*-butylamino)[60]fullerene as shown in the insert of Fig. 9. Therefore, by assuming a low absorption of *n*-butylamino functional moieties in the UV–VIS range, the spectrum of hexa(*n*-butylamino)[60]fullerene can quantitatively account for the molar optical absorbance of the organoaminated C_{60} moiety and can be utilized as a reference in the determination of the number of oligoanilino arms in the structure of starburst fullerene derivatives.

The shoulder band of Fig. 9b became much more pronounced when the chain length of star-arms extends to that of **3**, coherent with a rapid increase of the relative absorption intensity due to the π–π* transition of dianilino (–NH–B–NH–B) moieties at 289 nm (Fig. 10b). No optical absorption due to the presence of the quinonoid (–N=Q=N–) unit was observed at 500–650 nm[36] and this indicated a high purity of the reduced B-form of dianilino arms in the structure of **3**. Interestingly, even with a mixture of the B-form and Q-form of dianiline[37] in a ratio of roughly 1 : 1 used in the substitution reaction of $C_{60}(NO_2)_6$ for the preparation of **3**, a nearly identical optical spectrum of products as that of Fig. 10b was obtained. This revealed a much lower nucleophilic reactivity of the oxidized Q-form of dianiline towards fullerenic nitro groups, as compared with its B-form.

The π–π* transition band of the reduced oligoanilino moieties was found to increase progressively in intensity as the star arms were changed from dianilino to tetraanilino and hexadecaanilino groups leading to the starburst compounds of HTAF (Fig. 10d) and HHDAF (Fig. 10e), respectively. The same molar concentration of sample solution was used in all UV–VIS experiments, except PANI. A slight red shift of the peak maximum was detected from 289 nm for **3** to a longer wavelength of 303 and 317 nm for **4** and **5**, respectively. The latter is in a similar range as that of hexadecaaniline (317 nm, Fig. 10c) and PANI (323 nm, Fig. 10f). Formation of the quinonoid structure in the emeraldine base form of hexadecaaniline, HTAF, and HHDAF was evident showing a new band[36] centered at 578, 548, and 586 nm, respectively. A close similarity of the quinonoid absorption maximum between HHDAF and high molecular weight polyaniline (590 nm, Fig. 10f), showing only a 4 nm blue shift, may support our approach to reproduce the optical properties of PANI with the readily soluble starburst macromolecule of HHDAF.

Correlation of the total UV–VIS spectral area count of HAF, HDAF, HTAF, and HHDAF to the variation of sample concentration in THF was studied. An approximately linear relationship for all samples was obtained in the concentration range of $1.0–6.0 \times 10^{-6}$ M. At this concentration range, aggregation of the starburst molecules forming a nano-particle is unlikely. Owing to the strong optical absorption of the quinonoid moiety, the photon absorbance count of **4** and **5** increases accordingly in response to the increase of the sample concentration in a nearly identical rate. This rate is faster than the corresponding rate for **2** and **3** with a steeper slope for the fitted correlation line. We evaluated the possibility for utilizing this linear photon absorbance correlation to estimate the number of oligoanilino arms per C_{60} molecule in the composition of anilinated and oligoanilinated fullerenes. In principle, the compounds **2** and **3** consisting of a higher percentage content of the C_{60} moiety should facilitate a better differentiation of optical absorbance changes upon variation of the number of addends. Accordingly, a sample of HDAF was utilized as a model for the study. In measurements of the UV–VIS spectrum, the quantity of **3** used was derived from the assumption of its molecular formula as either $C_{60}(\text{dianiline})_5$, $C_{60}(\text{dianiline})_6$, or $C_{60}(\text{dianiline})_7$ to give the same concentration of a sample solution (2.5×10^{-6} M in THF). The total absorbance count of each of these three spectra was deducted by the percentage molar absorbance of the C_{60} moiety, obtained from Fig. 9a and the molar content of the C_{60} moiety in the assumed molecular formula. The remaining absorbance count corresponds to the total optical contribution of all dianilino arms. The optical absorbance of a single dianilino arm in the same molarity can be measured separately. From this operation, the number of dianilino addends per C_{60} was obtained as (with the percentage deviation indicated) 6.0 (+20%), 6.5 (+8.3%), and 9.2 (+31.4%) for the assumed molecular formula of $C_{60}(\text{dianiline})_5$, $C_{60}(\text{dianiline})_6$, and $C_{60}(\text{dianiline})_7$, respectively. These results revealed that the lowest deviation of the absorbance correlation was obtained by adopting the molecular formula of **3** as $C_{60}(\text{dianiline})_6$, containing 6 addends consistent with other spectral measurements. By using the same experimental procedure, the number of hexadecaanilino arms was obtained as 6.4 for the composition of HHDAF **5** in a similar range of experimental error.

Finally, oligoanilinofullerenes **3**–**5** showed appreciable fluorescence (FL) characteristics upon photo-excitation. In the case

of HAF, the energy relaxation of the photo-excited C_{60} moiety under either 250 or 300 nm irradiation gave a fluorescence band centered at 349 or 362 nm, respectively. As the number of anilino units in each arm increased for **4** and **5**, the fluorescence response contributed from the oligoanilino moiety in its emeraldine base form tends to dominate the FL spectrum. Consequently, a major fluorescence peak centered at 415 or 418 nm derived from the photo-excitation of oligoanilino arms under irradiation at either 250 or 300–350 nm, respectively, was detected along with a minor relaxation band of the excited C_{60} moiety at 350 nm in a much lower intensity.

Conclusion

A facile synthesis of starburst hexaanilino, hexa(dianilino), hexa(tetraanilino), and hexa(hexadecaanilino)[60]fullerenes was demonstrated using hexanitro[60]fullerene (HNF) as a reactive precursor molecule. Hexanitro[60]fullerene was prepared by direct nitration of the C_{60} molecules using gaseous nitrogen dioxide as the nitration agent. Negative ion DCI-MS spectra of hexaanilino[60]fullerene and hexanitroso[60]-fullerene, a hydride-reduced product of HNF, were utilized for substantiation of the number of addends per C_{60} in these fullerene derivatives. Detection of the molecular ion of $C_{60}(NO)_6$ at *m*/*z* 901 was correlated to the composition of its parent compound HNF, containing 6 nitro addends per C_{60} cage. The tertiary nitro groups of nitrofullerene compounds can be located at allylic or benzylallylic carbon atoms in the structure of HNF. This type of nitro function was found to act as an excellent leaving group for replacement by a nucleophilic substituent. Utilizing this reactivity with electron-donor nucleophiles, a synthetic approach was developed for producing oligoanilinated fullerenes as intramolecular donor–acceptor A–$(D)_6$ starburst macromolecules with a well-defined arm number and chain length. The chemistry can also be generalized in the preparation of organo-amino derivatives of C_{60} as a versatile alternative synthetic method for indirect fullerene functionalization and grafting onto polymers. Reactivity of HNF with oligomeric anilines increases with the increasing number of the repeating aniline units. Therefore, only an equal molar quantity of tetraaniline and hexadecaaniline was necessary for a complete reaction with HNF under mild conditions. Various spectroscopic methods were utilized in the characterization of hexa(oligoanilino)[60]fullerene products. One method for determining the number of addends per C_{60} molecule in the composition of the fullerene derivatives was developed using the quantitative measurement of the materials proton count *via* the proton integration over its ^{1}H NMR spectrum. As a result, the NMR data fits well with the structure of tetraanilinated and hexadecaanilinated fullerenes, containing 6 tetraanilino and hexadecaanilino arms per C_{60}, respectively. This composition of **5** was also supported by the DCI^--MS spectroscopic data which showed an approximated correlation of the total relative peak intensities of fragmented oligoanilino mass ion groups detected in the spectrum. Based on the nature of the nucleophilic substitution reaction of **1** with oligoanilines, all hexa-(oligoanilinated) fullerene products of **2**, **3**, **4**, and **5** are likely to consist of a number of hexa-adduct regioisomers.

An emeraldine base form containing quinonoid units is the thermally stable structure of each oligoanilino arm attached on C_{60}. Chemical reduction of HTAF and HHDAF with hydrazine (Scheme 1) in a solvent mixture of EtOH and DMF at ambient temperature gave the corresponding fully reduced products **8** and **9**, respectively. Upon exposure of HTAF and HHDAF in a fully reduced form to the air, regeneration of the quinonoid units along the oligoaniline chain leading to the emeraldine base structure of HTAF **4** and HHDAF **5** was observed as expected. The optical properties of hexa(hexadecaanilino)[60]-fullerenes revealed a close similarity with that of polyanilines in a high molecular weight and may suggest the possibility of generating promising conductive and photo-induced electron-transfer properties with this new class of starburst macromolecules.

Experimental

Pure C_{60} was purchased from either Bucky USA or Southern Chemical Co. and used as received. Infrared spectra were recorded as KBr pellets on a Nicolet 750 series FT-IR spectrometer. ^{1}H NMR spectra were recorded on either a Varian Gemini-200 spectrometer or Bruker AC-300 spectrometer. UV–VIS spectra were recorded on a Hitachi U-3410 UV spectrometer. HPLC analyses were performed on a Waters Delta Prep. 4000 HPLC system equipped with a Waters 486 UV detector operated at 340 nm, controlled and processed by Millinum software. A reverse-phase MCH-5 column (Varian Instruments, 2 × 300 mm) was used for the analysis using CH_3CN as eluent at a flow rate of 0.6 ml min^{-1}. Thermogravimetric analyses (TGA) data were collected on a thermogravimetric analyzer 2950 of TA Instruments with a heating rate of 10 °C min^{-1}. Benzene and toluene were dried and distilled over Na. Both sodium nitrite and nitric acid were purchased from Merck Inc.

Mass spectroscopic studies were performed by use of either the positive ion fast atom bombardment (FAB^+) technique with a direct probe on a JEOL JMS-HX110 high performance mass spectrometer or the negative ion desorption chemical ionization (DCI^-) technique with a direct probe on a JEOL JMS-SX102A mass spectrometer at National Tsing-Hwa University, Taiwan. Both the negative ion matrix-assisted laser desorption ionization ($MALDI^-$) and the positive ion laser desorption ionization (LDI^+) mass spectrum were recorded on a HP G2025A MALDI-TOF MS system. A N_2-laser operated at a wavelength of 337 nm was utilized for providing a dissociation energy of roughly 2.5 mJ in the negative ion measurements. The concentration of compound in a sample solution deposited on a MALDI probe was roughly 1000 ppm. Elemental analyses of fullerene derivatives were carried out at either the Institute of Nuclear Energy Research, Taiwan or the E + R Microanalytical Laboratory, Inc., Corona, New York.

Synthesis of hexaanilino[60]fullerene (HAF) 2

A reported procedure was applied in the preparation of **2**.[29]

Synthesis of hexa(dianilino)[60]fullerene (HDAF) 3

In a dry flask with a stirring bar, hexanitro[60]fullerene[29,30] (0.1 g, 0.1 mmol) dissolved in THF (5.0 ml) was charged under N_2. To this orange-colored solution, *N*-(phenyl)phenylene-1,4-diamine (2.3 g, 12.5 mmol, 125 equiv.) in dry THF (10 ml) was added, followed by triethylamine (2.0 g). The reaction mixture turned brown immediately. It was stirred at 50 °C for 6.0 h under nitrogen. At the end of the reaction, it was quenched with a mixture of water, THF and ethyl acetate. The organic layer (THF and ethyl acetate) was washed three times with brine and then dried over anhydrous Na_2SO_4. Most of the solvents were removed and the resulting viscous mass was added with a mixture of chloroform and hexane (1 : 1, 30 ml) causing precipitation of the products. The dark brown precipitates were washed with a solvent mixture of chloroform and hexane until no starting *N*-(phenyl)phenylene-1,4-diamine was detectable on TLC. The solids were then dried under vacuum at 40 °C and purified by preparative TLC (SiO_2, THF–$CHCl_3$/1 : 1) to yield hexa(dianilino)[60]fullerene **3** (0.14 g, 76%). IR ν_{max} (KBr) 3395 (br, N–H), 3039 (C–H), 1597, 1510 (s), 1495 (s), 1311, 1242, 1183, 1038, 828, 749, 703, and 512 cm^{-1}; UV–VIS (THF, 2.5×10^{-6} M): λ_{max} 222, 240 (shoulder), and 289 nm. Anal. Calcd for $C_{132}H_{86}N_{12}O_{10}$ as $C_{60}(NHC_6H_4NHC_6H_5)_6 \cdot 10H_2O$: C, 79.28; H, 4.30; N, 8.41; O, 8.01. Found: C, 78.70; H, 4.10; N, 9.02; O, 8.18% (by difference).

Synthesis of hexa(tetraanilino)[60]fullerene (HTAF) 4

In a dry flask with a magnetic stirring bar, hexanitro[60]fullerene (0.39 g, 0.39 mmol) dissolved in THF (10 ml) was charged under N_2. To this solution, tetraaniline (1.03 g, 2.82 mmol, 7.2 equiv.) in dry THF (15 ml) was added, followed by triethylamine (3.0 g). The deep blue-colored reaction mixture was stirred at 50 °C for 6.0 h and quenched by the addition of water and THF. The organic layer was then washed three times with brine and dried over anhydrous Na_2SO_4. After removal of most of the solvents, the dark blue products were precipitated upon the addition of ether (50 ml). The precipitates were filtered and washed with ether until no blue coloration in the washings was observed. The solids were then dried in vacuum at 40 °C and purified by preparative TLC [SiO_2, $R_f = 0.1$ using THF–$CHCl_3$ (1 : 1) as eluent] to yield hexa(tetraanilino)[60]fullerene **4** (0.82 g, 72%). IR ν_{max} (KBr) 3381 (br, N–H), 3031 (C–H), 1596, 1509 (s), 1303, 1245, 1171, 1071, 828, 748, 694, and 501 cm^{-1}; UV–VIS (THF, 2.5×10^{-6} M): λ_{max} 303 and 548 nm. Anal. Calcd for $C_{204}H_{138}N_{24}O_{12}$ as $C_{60}(NHC_6H_4NC_6H_4NC_6H_4NHC_6H_5)_6 \cdot 12H_2O$: C, 78.62; H, 4.45; N, 10.79; O, 6.17. Found: C, 77.42; H, 4.13; N, 10.90; O, 7.55% (by difference).

Synthesis of hexa(hexadecaanilino)[60]fullerene (HHDAF) 5

In a dry flask purged with nitrogen, hexanitro[60]fullerenes (0.11 g, 0.11 mmol) dissolved in THF (5.0 ml) was charged under N_2. To this solution hexadecaaniline (0.96 g, 0.66 mmol, 6.0 equiv.) in dry THF (20 ml) was added followed by triethylamine (3.0 g). To enhance the solubility of the products in solution, *N*-methylpyrrolidinone (7.0 ml) was also added. The deep violet-colored reaction mixture was stirred at 50 °C for 24 h. At the end of reaction, THF was removed by rotary evaporation. The remaining black-colored solution was poured into water (40 ml) causing precipitation of the products. The dark violet-colored precipitates were washed several times with water (10 ml each) and filtered. The solids were further washed several times with acetonitrile (10 ml each) for removal of unreacted hexadecaaniline until no violet color showed in the washings and dried under vacuum at 40 °C to afford hexa(hexadecaanilino)[60]fullerene **5** (0.98 g) in 94% yield. Chromatographic purification of **5** was performed on TLC [SiO_2, $R_f = 0.8$ for hexadecaaniline **7** and $R_f = 0.1$ for **5** using THF–$CHCl_3$ (1 : 1) as eluent or $R_f = 0.9$ for **7** and $R_f = 0.2$ for **5** using THF–$CHCl_3$ (3 : 1) as eluent]. IR ν_{max} (KBr) 3407 (br, N–H), 2934 (C–H), 2855, 1658, 1594, 1507 (s), 1303, 1262, 1183, 1143, 1051, 824, 755, 696, and 508 cm^{-1}; UV–VIS (THF, 2.5×10^{-6} M): λ_{max} 229, 317, and 584 nm. Anal. Calcd for $C_{636}H_{552}N_{96}O_{48}$ as $C_{60}[(NHC_6H_4NC_6H_4NC_6H_4NHC_6H_5)_4]_6 \cdot 48H_2O$: C, 74.13; H, 5.36; N, 13.05; O, 7.46. Found: C, 74.3; H, 5.2; N, 12.4; O, 8.1% (by difference).

DCI^--MS of **5** *m*/*z* (with the relative percentage intensity indicated) 721 (C_{60}, 85.1), 548 ($n = 6$, 18.5), 637 ($n = 7$, 22.3), 728 ($n = 8$, 30.4), 820 ($n = 9$, 54.7), 912 ($n = 10$, 71.6), 1003 ($n = 11$, 80.5), 1093 ($n = 12$, 67.6), 1185 ($n = 13$, 80.8), 1276 ($n = 14$, 29.9), 1367 ($n = 15$, 16.6), and 1459 ($n = 16$, 12.5) for hexadecaaniline ions, $H(C_6H_4NH)_n^-$; also *m*/*z* 561 ($n = 6$, 28.5), 653 ($n = 7$, 38.2), 744 ($n = 8$, 47.5), 835 ($n = 9$, 71.5), 927 ($n = 10$, 100), 1018 ($n = 11$, 70.6), 1110 ($n = 12$, 43.8), 1200 ($n = 13$, 26.5), 1292 ($n = 14$, 20.6), 1383 ($n = 15$, 14.1), and 1475 ($n = 16$, 10.9) for $HN(C_6H_4NH)_nH^-$ ions.

Acknowledgements

We thank Dr Jentaie Shiea of National Sun Yat-Sen University, Taiwan for the collection of MALDI-MS data and Mr S. J. Wang of the Instrumentation Center at National Tsing-Hwa University, Taiwan for the collection of FAB and DCI mass data.

References

1 A. W. Jensen, S. R. Wilson and D. I. Schuster, *Bioorg. Med. Chem.*, 1996, **4**, 767.
2 Q. Zheng, R. Sun, X. Zhang, T. Masuda and T. Kobayashi, *Jpn. J. Appl. Phys.*, 1997, **36**, 1675.
3 J. McElvain, M. Keshavarz, H. Wang, F. Wudl and A. J. Heeger, *J. Appl. Phys.*, 1997, **81**, 6468.
4 Y. Tajima, Y. Tezuka, T. Ishii and K. Takeuchi, *Polym. J.*, 1997, **29**, 1016.
5 Y. Kojima, T. Matsuoka, H. Takahashi and T. Kurauchi, *Macromolecules*, 1995, **28**, 8868.
6 G. Yu, J. Gao, J. C. Hummelen, F. Wudl and A. J. Heeger, *Science*, 1995, **270**, 1789.
7 S. V. Frolov, P. A. Lane, M. Ozaki, K. Yoshino and Z. V. Vardeny, *Chem. Phys. Lett.*, 1998, **286**, 21.
8 E. T. Samulski, J. M. DeSimmone, M. O. Hunt, Jr., Y. Z. Menceloglu, R. C. Jarnagin, G. A. York, K. B. Labat and H. Wang, *Chem. Mater.*, 1992, **4**, 1153.
9 Y. Chen, W. S. Huang, Z. E. Huang, R. F. Cai, H. K. Yu, S. M. Chen and X. M. Yan, *Eur. Polym. J.*, 1997, **33**, 823.
10 Y. Ederle and C. Mathis, *Macromolecules*, 1997, **30**, 2546.
11 M. M. Khaled, R. T. Carlin, P. C. Trulove, G. R. Eaton and S. S. Eaton, *J. Am. Chem. Soc.*, 1994, **116**, 3465.
12 C. J. Hawker, K. L. Wooley and M. J. Frechet, *J. Chem. Soc.*, *Chem. Commun.*, 1994, 925.
13 E. Cloutet, Y. Gnanou, J. L. Fillaut and D. Astruc, *Chem. Commun.*, 1996, 1565.
14 L. Y. Chiang, L. Y. Wang, S. M. Tseng, J. S. Wu and K. H. Hsieh, *J. Chem. Soc.*, *Chem. Commun.*, 1994, 2675.
15 Y. Ederle and C. Mathis, *Macromolecules*, 1997, **30**, 4262.
16 C. E. Bunker, G. E. Lawson and Y. P. Sun, *Macromolecules*, 1995, **28**, 3744.
17 T. Cao and S. E. Webber, *Macromolecules*, 1996, **29**, 3826.
18 W. T. Ford, T. D. Graham and T. H. Mourey, *Macromolecules*, 1997, **30**, 6422.
19 L. Y. Chiang, L. Y. Wang, S. M. Tseng, J. S. Wu and K. H. Hsieh, *Synth. Met.*, 1995, **70**, 1477.
20 L. Y. Chiang, L. Y. Wang and C. S. Kuo, *Macromolecules*, 1995, **28**, 7574.
21 F. Wang, R. D. Rauch and T. L. Rose, *J. Am. Chem. Soc.*, 1997, **119**, 11106.
22 A. D. MacDirarmid and A. J. Epstein, *Faraday Discuss.*, *Chem. Soc.*, 1989, **88**, 317.
23 E. M. Genies, A. Boyle, M. Lapkowski and C. Tsintavis, *Synth. Met.*, 1990, **36**, 139.
24 F. L. Lu, F. Wudl, M. Nowak and A. J. Heeger, *J. Am. Chem. Soc.*, 1986, **108**, 8311.
25 J. M. Ginder, A. J. Epstein, R. W. Bigelow, A. F. Richter and A. G. MacDiarmid, *Bull. Am. Phys. Soc.*, 1986, K17.
26 Y. Wei, C. Yang and T. Ding, *Tetrahedron Lett.*, 1996, **37**, 731.
27 W. J. Zhang, J. Feng, A. G. MacDiarmid and A. J. Epstein, *Synth. Met.*, 1997, **84**, 119.
28 *The Chemistry of Fullerenes*, ed. R. Taylor, World Scientific, Singapore, 1995.
29 V. Anantharaj, J. Bhonsle, T. Canteenwala, L. Y. Chiang, *J. Chem. Soc.*, *Perkin Trans. 1*, 1999, 31.
30 L. Y. Chiang, J. B. Bhonsle, L. Y. Wang, S. F. Shu, T. M. Chang and J. R. Hwu, *Tetrahedron*, 1996, **52**, 4963.
31 F. Wudl, A. Hirsch, K. C. Khemani, T. Suzuki, P. M. Allemand, A. Koch, H. Eckert, G. Srdanov and H. M. Webb, *ACS Symp. Ser.*, 1992, **481**, 161.
32 A. Hirsch, Q. Li and F. Wudl, *Angew. Chem.*, *Int. Ed. Engl.*, 1991, **30**, 1309.
33 Z. Slanina, T. Sugiki, L. Y. Chiang and E. Osawa, in *Fullerenes*, vol. 5, eds. R. S. Ruoff and K. S. Kadish, The Electrochem. Soc., Pennington, NJ, 1997, p. 167 and 721.
34 X. Zhao, Z. Slanina, L. Y. Chiang and E. Osawa, in *Fullerenes*, vol. 6, eds. R. S. Ruoff and K. S. Kadish, The Electrochem. Soc., Pennington, NJ, 1998, p. 130.
35 L. Y. Wang, V. Anantharaj, K. Ashok and L. Y. Chiang, *Synth. Met.*, 1999, **103**, 2350.
36 Y. Cao, P. Smith and A. J. Heeger, *Synth. Met.*, 1989, **32**, 263.
37 ^1H NMR spectrum showed a mixture of the B-form and Q-form of dianilines in a ratio of roughly 1 : 1; the B-form δ 4.54 (s, 2H), 6.50 (d, 2H), 6.54 (t, 1H), 6.75 (d, 2H), and 6.83 (d, 4H). The Q-form δ 6.50 (d, 2H), 6.54 (t, H), 6.75 (d, 2H), 7.05 (d, 2H), 7.11 (d, 2H), and 7.44 (s, 1H).

Paper 9/05393J